1. Karol ŚWIERCZYŃSKI, 2. Marcin HABRYCH, 3. Bartosz BRUSILOWICZ

ORCID: 1. 0000-0001-5897-0358; 2. 0000-0003-2067-0135, 3. 0000-0002-4113-2689

OPEN ACCESS

Coordination of ROCOF and frequency elements in power systems with high penetration of distributed generation

Koordynacja członów ROCOF i częstotliwościowych w systemach elektroenergetycznych z dużym rozpowszechnieniem generacji rozproszonej

Abstract. *This article presents various methods for calculating frequency deviations in response to changes in parameters affecting the operation of the power system, such as load, power flows, distributed generation, and inertia. The paper also includes a comprehensive analysis of frequency disturbance tests conducted under different scenarios, evaluating the performance and response of power system protection mechanisms. By studying the impact of these disturbances on system stability and the operation of protective devices, the paper provides insights into the critical role of Rate of Change of Frequency (ROCOF) calculation in ensuring the reliability and resilience of electrical grids. The findings highlight the importance of accurate ROCOF calculations and robust protection schemes to mitigate potential system failures.*

Streszczenie. *W artykule przedstawiono różne metody obliczania zmian częstotliwości w odpowiedzi na zmiany parametrów wpływających na pracę systemu elektroenergetycznego, takich jak obciążenie, przepływy mocy, generacja rozproszona i inercja. Artykuł zawiera również kompleksową analizę testów zaburzeń częstotliwości przeprowadzonych w różnych scenariuszach, oceniających wydajność i reakcję zabezpieczeń częstotliwościowych. Badając wpływ tych zakłóceń na stabilność systemu i działanie urządzeń zabezpieczających, artykuł dostarcza wglądu w krytyczną rolę obliczeń szybkości zmian częstotliwości w czasie (ROCOF) w zapewnianiu niezawodności pracy systemu elektroenergetycznego. Wyniki badań podkreślają znaczenie dokładnych obliczeń ROCOF i stosowania pewnych zabezpieczeń częstotliwościowych w celu złagodzenia potencjalnych awarii systemowych.*

Keywords: distributed generation, frequency protection, island operation, ROCOF, synchronous generator.
Słowa kluczowe: generacja rozproszona, zabezpieczenia częstotliwościowe, praca wyspowa, ROCOF, generator synchroniczny.

Introduction

Over the past decades, there has been a definite development in renewable energy sources. A growing amount of distributed generation is installed in the electric power system [1]. Distributed generation has an increasing impact on the operation of the power system. Especially, the values of voltage or its frequency may rapidly change [2], [3]. The increase in installations also leads to phenomena that have not previously occurred in power systems. However, it also creates new opportunities that, shaped appropriately, can be useful in aspects of ensuring the power system stability. The article presents one aspect of integrating distributed generation into the system: the analysis of the impact of distributed generation on frequency changes.

Many documents describe frequency protection requirements; for instance, in Europe, the requirements are in documents issued by ENTSO-E (European Network of Transmission System Operators for Electricity) [4]. According to [3], load-shedding automation should be executed using underfrequency relays and those responding to the rate of change of frequency (ROCOF). What is more, the authors of [5] have developed an underfrequency load-shedding scheme based on ROCOF measurements and a static-voltage stability estimation. The implementation of this algorithm may allow the mitigation of frequency deviations during system disturbances.

Another interesting issue is the inverse dependence of the rate of change of frequency on the total inertia of the system [6]. The lower the inertia of a given section of the grid - for example, in the case of a high dissemination of inverter-based resources, such as photovoltaic or wind farms - the higher the value of ROCOF can be expected. In addition, the European power system should remain stable with a power imbalance of about 40%, which may correspond to a rate of frequency change of 2 Hz/s [6].

The operation of the ROCOF criterion is accompanied by certain technical problems. The first is related to the non-detection zone (NDZ), i.e., the zone in which the protective relay may trip or may not trip [7]. Throughout the isolation of an island with a relatively precise power balance, the ROCOF relays may have problems identifying this incident [8]. The detection time may increase, thereby reducing the security of the grid operation [9]. Additionally, the islanding process cannot be detected in the case of an almost ideal power balance [10]. The articles [11], [12] present the scrutiny related to the accuracy of island detection in different active and reactive power balance scenarios. Their authors demonstrated that the tripping time of the ROCOF criterion decreases in compliance with the increase of active power imbalance. Some research papers have described the operation problem of the ROCOF criterion. The papers present additional methods to calculate frequency and ROCOF precisely, e.g., using maximum likelihood frequency and ROCOF estimator [13], [14]. Another approach is to use additional criteria, e.g., by adding small signals to the inverter's modulation indexes to cause voltage disturbances at the Point of Common Coupling (PCC), where the ROCOF is monitored [15], or by monitoring voltage waveform to detect step changes of its parameters [16].

The crucial issue related to ROCOF calculations is energy production's large share of inverter-based resources (IBRs). The IBRs are characterized by almost zero inertia; therefore, the frequency changes during events in the power system may be rapid. This phenomenon is known as fast frequency response (FFR) [17]. There are several strategies to control sources, such as photovoltaics and wind turbines, to mitigate FFR: synthetic inertia [18], emulated inertia [19], or virtual inertia [20].

The ROCOF criterion is most widely utilized in island detection [21]. In this application, the critical issue is the estimation of ROCOF value. The obtained rate of change of frequency and, consequently, the detection effectiveness depends on the chosen time window. For example, the shorter the measurement window, the higher the value of ROCOF [22]. Moreover, a large window size tends to filter high-speed oscillations and displace the time of the maximum instantaneous ROCOF [23]. The important issue is also the type of measurement window. In [23], the authors

propose the utilization of a rolling window and illustrate the benefits of its use over a fixed window. Another approach is using more than one window with different sizes and multiple thresholds to detect an ROCOF event [24].

Furthermore, the described criterion might also be utilized in power system stability determining, for example, center of inertia (CoI) calculations [25]. The inertia can be calculated using mathematical formulas presented in [26] for different types of power systems, including photovoltaic-based distribution systems. This information can be further utilized in different control algorithms for IBRs [27].

The authors of this article focused on other properties and applications of the ROCOF criterion. Especially on the measurements of ROCOF during island isolation in the medium voltage grids with a large share of inverter-based resources. The conducted research is related to the tests of variability of frequency in different system scenarios. These conditions have been adapted to the phenomena occurring in the Continental European Power System [28]. During the tests, the power flows, the generator parameters, such as inertia or damping factor, and the types of loads were varied. In contrast to the cited research papers, the power imbalance during simulations was changed in both directions, i.e., power deficiency and power exceedance. In addition, the authors have also examined the sensitivity of the power system protection utilized in the Continental European Power System on frequency deviations. Different protection criteria, such as under- and overfrequency or ROCOF, were tested in this aspect. Throughout the tests, the protection settings and frequency disturbances were changed.

The conducted research proved that the value of ROCOF is affected by many parameters describing the devices installed in the power system. Thus, the operation of the power system protection might be susceptible to these changes. The exemplified analysis of the coordination of frequency elements is the main contribution of this article and introduces a novel approach to the ROCOF estimation. Moreover, the latest literature emphasizes the importance and actuality of this topic.

Theoretical analysis

The supply voltage frequency is one of the most important parameters describing the operation of the power system. The frequency is closely related to the balance of active power - when there is an excess of generated power over the power of loads, the frequency increases, while when there is a shortage of generated power, the frequency decreases. This phenomenon is related to synchronous generators' operating characteristics and control systems. The following analysis can be used for both 50 Hz and 60 Hz power systems. A simplified model of the relationship between generated power and synchronous generator speed is described in Figure 1 [29].
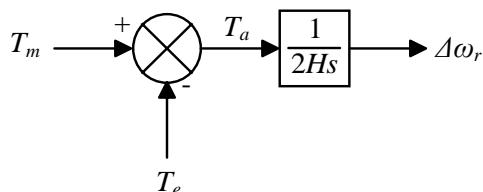
Fig. 1. The relationship between the change in speed and the change in the load torque of the synchronous generator

Parameters T_m, T_e, and T_a are the values of the mechanical torque supplied to the machine, the electric torque, and the resultant torque, respectively, usually expressed per unit. Changing the resultant torque considering the inertia of the machine H expressed in seconds causes a change in the

rotor speed of the generator $\Delta\omega_r$, and consequently the frequency of the generated voltage. The rotational speed and torque can be used to calculate the power (1) [29]

$$(1) \qquad P = \omega_r T$$

Assuming a steady-state speed ω_r = 1pu, we can write formula (2) [29]. The block diagram considering (2) is shown in Figure 2.

$$(2) \qquad \Delta P_m - \Delta P_e = \Delta T_m - \Delta T_e$$
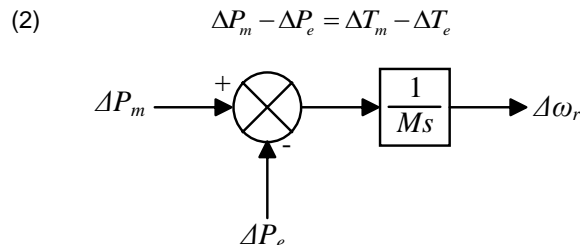
Fig. 2. The relationship between the change in speed and the change in the load power of the synchronous generator, where $M=2H$

Based on the block diagram presented above, it is possible to calculate the impact of load or mechanical power changes on the frequency change in the network. Considering the step change in electrical power ΔP_e, we get the frequency change relation in the frequency domain (3) [29].

$$(3) \qquad \Delta\omega_r(s) = \frac{-\Delta P_e}{s} * \frac{1}{Ms}$$

Performing the inverse Laplace transform, the formula for a straight line that describes the relative change in rotor speed of a generator over time can be obtained (4) [29].

$$(4) \qquad \Delta\omega_r(t) = \frac{-\Delta P_e}{M}t$$

The slope of the linear function determines the rate of change in the speed of the generator. This coefficient depends in direct proportion to the changes in load power and inverse proportion to the inertia of the machine. Using the relationship $\omega = 2\pi f$, we obtain the formula for the straight line describing the change in frequency of the generated voltage in response to a change in load occurring in the grid.

However, the actual synchronous generator is a more complex system. Changes in the frequency of the generated voltage depend on the design of the machine. These changes are not only related to the dimensions of the generator or the utilized mechanical components but also to the electrical part of the generator - the windings. This aspect concerns the so-called damping windings. The damping windings impact the suppression of rapid changes in the rotor speed of the generator, which directly affects the rate of change of frequency [30]. The value of the damping coefficient K_D for a specific generator can be calculated from the rated parameters of the machine using formula (5) [30],

$$(5) \qquad K_D = \frac{E^2\left(x_d^{'} - x_d^{''}\right)T_{d0}^{''}s}{\left(x_d^{''}\right)^2 \omega}$$

where: E - rated voltage, $x_d^{'}$ - subtransient reactance in the direct axis, $x_d^{''}$ - subtransient reactance in the direct axis, $T_{d0}^{''}$ - open-circuit subtransient time constant in the direct axis, s - slip, ω - angular frequency.

In addition, the load-damping constant D has a similar effect on the change in rotor speed. This constant is

expressed as a percentage of load power change per 1% change in frequency. Typical values range from 1 to 2%. In particular, the D factor is essential for frequency-sensitive loads, such as electric drives.

Considering the suppression of changes in the rotor speed of the generator, resulting from both the use of damping windings (K_D - damping coefficient) and the application of load-damping constant D in the calculations affect the frequency waveform. The block diagram of the generator with the consideration of damping is shown in Figure 3.
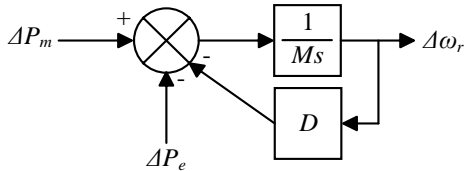
Fig. 3. The block diagram of a synchronous generator considering the damping factor

The changes in frequency cease to be linear, rapidly varying, and take on an exponential character, clearly moving toward some steady state [29]. This relationship is described by equation (6) [29] based on the above diagram, assuming a constant value of ΔP_m and a step change in ΔP_e.

$$(6) \qquad \Delta\omega_r(s) = \frac{-\Delta P_e}{s} * \frac{1}{Ms + D}$$

Considering in relation (6): $K = 1/D$ and $T = M/D$, and then performing the inverse Laplace transform, it can be obtained (7) [29]:

$$(7) \qquad \Delta\omega_r(t) = -\Delta P_e K e^{-\frac{t}{T}} + \Delta P_e K$$

which illustrates that frequency changes with damping coefficient have an exponential character.

Various types of control systems must be considered during the analysis of changes in the frequency of the generated voltage. For the purpose of this article, the authors focused on simple regulators of the generator rotor speed and generator excitation voltage. The implementation of the generator rotor speed regulator is shown in Figure 4, where ΔY – change of the valve position, P_m – mechanical power, P_e – electrical power, ω_0 – nominal speed, ω_r – current speed, $\Delta\omega_r$ – change of the speed. Using a speed regulator allows the rotational speed to be kept within the rated limit, and consequently, the rated frequency value of f = 50 Hz is maintained. The generator excitation voltage regulator has a similar structure. The difference is only in the controlled signals.
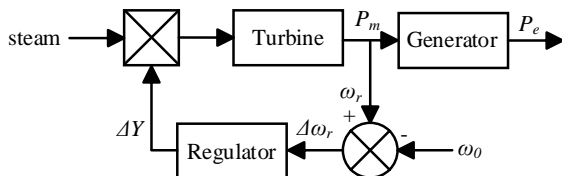
Fig. 4. The block diagram of the rotor speed control system

Turbine and excitation regulators typically have significant time constants relative to the operating times of protection relays. For this reason, the value and rate of change of frequency (ROCOF) measured by frequency criteria are affected by the mechanical parameters of the generators, particularly their inertia.

The simulations
Unidirectional power flow

A simulation study was conducted to determine the effect of changing various parameters describing the operation of synchronous generators (inertia H and damping D) and the effect of load changes (ΔP_e) on the change in the frequency of the generated voltage. Using MATLAB Simulink, a simplified synchronous generator model was prepared based on the block diagram shown in Figure 3.

During the first stage of the conducted simulations, the authors focused on checking the performance of a small synchronous generator with apparent power S = 1 MVA, voltage U = 400 V, and inertia H = 0.28 s at the value of the damping factor D = 0 %, without additional control systems. An example of the waveform of frequency changes resulting from the disconnection of the load is shown in Figure 5. It can be observed that the waveform, as expected, is linear. In this case, the value of ROCOF is 2 Hz/s. In contrast, the relative change in load ΔP_e is about 2.5%. The obtained result is consistent with the formulas in the previous section.

The second stage was to verify the cases considering damping resulting from both the load and the generator design. In the case of the modeled generator using equation (5), the damping factor K_D = 1% was calculated. As mentioned earlier, the D coefficient associated with frequency deviation-sensitive loads is selected from a range of 1-2%. Figure 6 shows the waveform of frequency changes with $K_D = D$ = 1% coefficients. The exponential nature of the changes can be observed, tending towards a certain steady state. In the described case, the load change ΔP_e was about 5%. In Figures 5 and 6, the blue lines indicate the frequency limits at which it is still possible to regulate this parameter. Furthermore, this increase in frequency value might accompany large system disturbances [31]. The red line is the demand disconnection starting at the mandatory level for the power system of continental Europe [28].

The rate of change of frequency is also affected by the inertia of the generator. It is closely related to the design of the machine and its moment of inertia. The larger the machine, the greater the rotating mass, and thus, the greater the inertia - the accumulated kinetic energy. In the next stage of the study, the effect of changing the inertia of the modeled generator on the frequency waveform was examined. For this purpose, the first case was modified with the parameters D = 0 %, H = 3 s, and ΔP_L = 2.5%. The obtained waveform is shown in Figure 7. In this case, the rate of change of frequency is significantly lower despite the disconnection of the load with the same power. According to the theory presented in the previous section, it can be concluded that the value of ROCOF is inversely proportional to the inertia of the generator H (4).
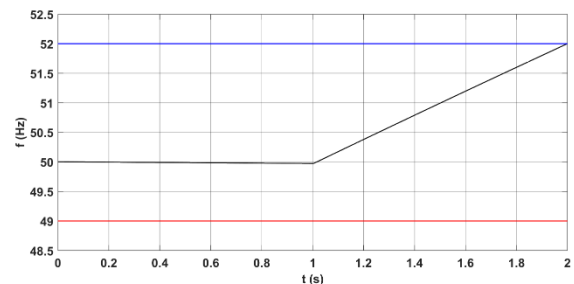
Fig.5. The frequency change in the grid caused by the disconnection of the load for D = 0%
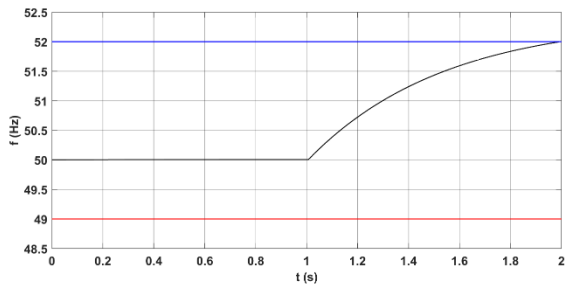
Fig.6. The frequency change in the grid due to disconnection of the load for D = 1%
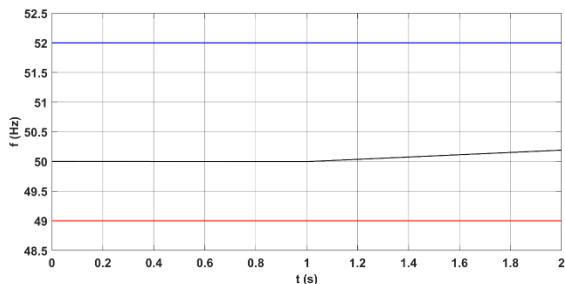
Fig.7. The frequency change in the grid due to disconnection of the load for H = 3 s and D = 0%

Bidirectional power flow

The rate of change of frequency (ROCOF) is an important parameter for detecting the island operation of generating units. A simulation study was conducted to determine how the change in load ΔP_e affects the change in frequency at the time of islanding. The model from the previous section was modified and adapted to the 20 kV rated voltage, representing a real medium voltage grid. Speed and excitation controllers enhanced the distributed synchronous generator model, reducing steady-state power oscillations [32]. The block representing a bulk power system with 2500 MVA short circuit power and 0,9 MVA PV power plant with a Grid Following control scheme was also implemented. A simplified block diagram of the modeled system is shown in Figure 8.
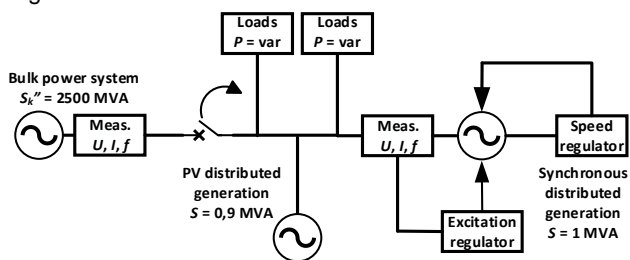
Fig.8. The block diagram of the tested simulation model

During the simulation, the separation of the island was modeled by switching off the circuit breaker (Fig. 8). The different cases of power balance were examined. The first instance is excess power in the separated island, i.e., the generated power is greater than the load power ($P_G > P_e$). The second is power deficiency in the separated island, i.e., the generated power is less than the load power ($P_G < P_e$). Throughout the tests, the inertia of the synchronous generator was set to $H = 2$ s, and the damping factor was set to $D = 0$ %. The frequency response of the PV power plant does not have inertia because of the control scheme that was implemented.

Figures 9 and 10 present examples of current flows during and after the islanding process in the case of excess generated power. At a steady state ($t = 0-2$ s), all three sources operate parallel and supply the 1,2 MW loads. PV

power plant energizes the MV grid with nominal power, a small synchronous generator operates with half of the nominal power, and a small excess of generated power is transferred to the power system. When the breaker is switched off ($t = 2$ s), the island is separated, and the distributed sources take over all the power of the loads. The generator current decreases (Fig. 9), whereas the current of photovoltaics remains constant (Fig. 10). During this process, the island is disconnected from the power system. Furthermore, Figure 11 shows the change in voltage frequency for this case. It is worth emphasizing that implementing different types of energy storage systems, such as electrochemical [33], mechanical [34], or thermal [35], can mitigate the frequency deviations in isolated islands [36].

Using the voltage waveforms obtained during simulation studies of various cases, COMTRADE files were generated and used further in laboratory tests.
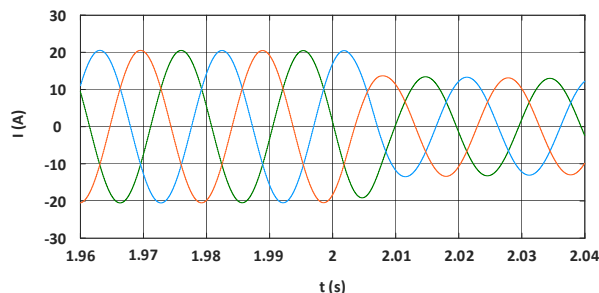
Fig.9. The generator current during isolation of an island with power excess
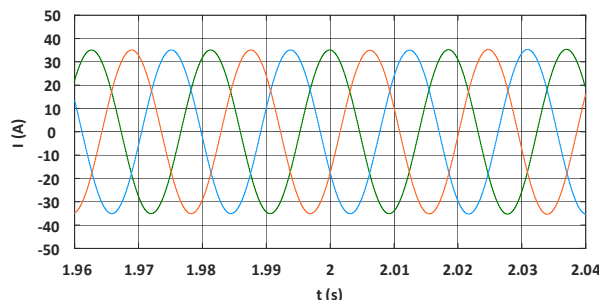
Fig.10. The PV power plant current during isolation of an island with power excess
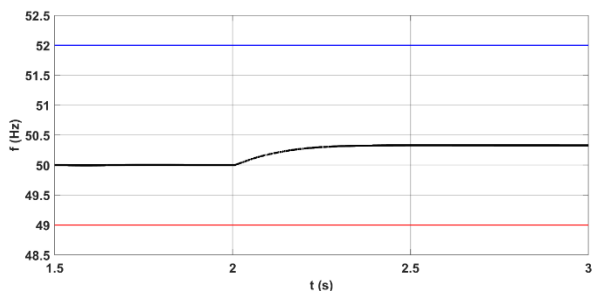
Fig.11. The change of the frequency during isolation of an island with power excess

The laboratory tests

Laboratory tests were conducted to verify the performance of frequency protection relays. A protection relay equipped with over- and underfrequency and ROCOF criteria was investigated. Using the Omicron CMC356 tester and COMTRADE type files generated from simulation studies, different variants of frequency changes were simulated. Furthermore, the response of the protection device, manufactured by one of the key companies on the

market, was verified. The block diagram of the measurement system is shown in Figure 12.

Typical for the European power system settings of frequency criteria were used during laboratory tests. According to the network code on requirements for grid connection of generators established by the European Commission, the settings for frequency relays should be defined by the proper Distribution System Operator [28], [37]. On the other hand, the American standard IEEE-1547 designates the ranges of setting groups for the under- and overfrequency criteria [38]. For the purpose of the tests, the different lengths of time delay for over- and underfrequency protection were examined. Moreover, in the case of the ROCOF criterion, the parameters of the measurement windows were varied. These settings have a significant effect on the tripping time of ROCOF protection. A summary of the settings of the tested frequency criteria is shown in Table 1. The settings of ROCOF's measurement windows were programmed to obtain a window with a short tripping time (about 250 ms) and a window with a long tripping time (about 750 ms). It must be emphasized that in the case of using the ROCOF criterion, time delays are not utilized. The time of its operation depends strongly on the measurement window settings.
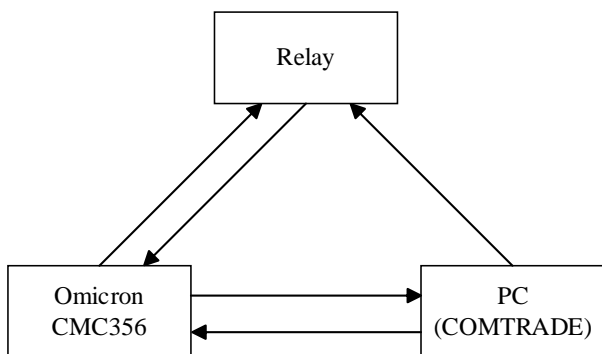
Fig.12. The block diagram of the measurement system

Table 1. The settings of frequency criteria

Criterion	Threshold	Time delay	
		Short	Long
Overfrequency 1st stage (f>)	50,5 Hz	0,3 s	1 s
Overfrequency 2nd stage (f>>)	51 Hz	0,2 s	0,5 s
Underfrequency 1st stage (f<)	49,5 Hz	0,5 s	1 s
Underfrequency 2nd stage (f<<)	49 Hz	0,2 s	0,5 s
ROCOF	2 Hz/s	0 s	0 s

The COMTRADE files used throughout the tests have contained different frequency variations resulting from active power excess or deficiency in the examined island. The results of this experiment were divided into two variants – increase (Table 2) and decrease (Table 3) of frequency. Each variant is described with four different settings combination:

1) Group 1 - Fast measurement window of ROCOF criterion and short time delay of frequency criterion,
2) Group 2 - Fast measurement window of ROCOF criterion and long time delay of frequency criterion,
3) Group 3 - Slow measurement window of ROCOF criterion and short time delay of frequency criterion,
4) Group 4 - Slow measurement window of ROCOF criterion and longtime delay of frequency criterion.

Table 2. The results of laboratory tests – frequency increase

Group	Criterion	Reaction
1	Overfrequency 1st stage (f>)	Pick-up
	Overfrequency 2nd stage (f>>)	-
	ROCOF	Trip
2	Overfrequency 1st stage (f>)	Pick-up
	Overfrequency 2nd stage (f>>)	-
	ROCOF	Trip
3	Overfrequency 1st stage (f>)	Trip
	Overfrequency 2nd stage (f>>)	-
	ROCOF	-
4	Overfrequency 1st stage (f>)	Pick-up
	Overfrequency 2nd stage (f>>)	-
	ROCOF	Trip

The impact of different setting groups and frequency variations on the protection response was examined during the tests. It can be concluded that the use of slow measurement windows of the ROCOF criterion results in the lack of response of this criterion to simulated frequency changes. In such cases, over- and underfrequency criteria with appropriate stages have proper conditions to trip. Moreover, utilizing setting groups with fast measurement window, the ROCOF criterion operates faster than under- or overfrequency criteria. Under these terms, the frequency criteria are only picked-up.

Table 3. The results of laboratory tests – frequency decrease

Group	Criterion	Reaction
1	Underfrequency 1st stage (f<)	Pick-up
	Underfrequency 2nd stage (f<<)	-
	ROCOF	Trip
2	Underfrequency 1st stage (f<)	Pick-up
	Underfrequency 2nd stage (f<<)	-
	ROCOF	Trip
3	Underfrequency 1st stage (f<)	Trip
	Underfrequency 2nd stage (f<<)	-
	ROCOF	-
4	Underfrequency 1st stage (f<)	Pick-up
	Underfrequency 2nd stage (f<<)	-
	ROCOF	Trip

Conclusion

Frequency protection is now required based on the provisions of various documents and legal acts. An important issue is their proper parameterization and selection for the specific cases. As shown in the article, frequency variations are affected by many factors. These are related to the parameters and/or design of the distributed source itself (inertia H, damping factor K_D), as well as to the loads installed deep in the network (damping factor D).

The rate of change of frequency is affected mainly by the inertia H of the source. The higher its value, the lower the dynamics of change. In addition, the damping resulting from the design of the generator and the character of the load installed in the grid also affects the rate of change of frequency. In the case of non-damping, the frequency changes have a fast-variable linear character, while when the damping increases, the changes assume an exponential character; the slower the variable, the greater the value of the damping factor is. When a distributed source is equipped with control systems, the frequency dynamics change depending on the devices used.

The properties of the distributed sources described above significantly impact the performance of frequency protections

installed in distribution grids. In addition, the performance of these protections is closely related to their settings. In the case of supplying the distribution system from sources with low inertia, such as IBRs, the ROCOF criterion can detect the frequency disturbances faster than standard frequency criteria. However, high inertia energy sources, such as synchronous generators, are characterized by slower frequency changes. Thus, in the case when their share is dominant, the standard underfrequency and overfrequency criteria might operate more reliably than the ROCOF criterion. Therefore, coordination of the mentioned protection elements should be well designed, considering the types of sources installed in the power system and their share in energy production. The analysis presented in the article can be used to achieve the reliable coordination.

Authors: *mgr inż. Karol Świerczyński, E-mail: karol.swierczynski@pwr.edu.pl; dr hab. inż. Marcin Habrych, prof. PWr, E-mail: marcin.habrych@pwr.edu.pl; dr inż. Bartosz Brusiłowicz, E-mail: bartosz.brusilowicz@pwr.edu.pl, Politechnika Wrocławska, Katedra Energoelektryki, ul. Janiszewskiego 8, 50-372 Wrocław.*

REFERENCES

[1] IRENA, "Reneweble Energy Statistic 2024," *Int. Renew. Energy Agency*, 2024, [Online]. Available: https://www.irena.org/Publications/2024/Mar/Renewable-capacity-statistics-2024.
[2] T. Bašakarad, N. Holjevac, I. Kuzle, I. ivanković, and N. Zovko, "Rocof Importance in Electric Power Systems With High Renewables Share: a Simulation Case for Croatia," pp. 72–77, 2021, doi: 10.1049/icp.2021.1239.
[3] ENTSO-E, "Inertia and Rate of Change of Frequency (RoCoF)," 2020.
[4] European Commission, "Commission Regulation (EU) 2017/1485: Establishing a guideline on Electricity Transmission System Operation (SO GL)," *Off. J. Eur. Union*, vol. L 220, no. 25 August 2017, p. 120, 2017, [Online]. Available: http://eur-lex.europa.eu/legal-content/EN/TXT/PDF/?uri=CELEX:32017R1485&from=EN.
[5] N. Al Masood, A. Jawad, and S. Banik, "A RoCoF-constrained underfrequency load shedding scheme with static voltage stability-based zoning approach," *Sustain. Energy, Grids Networks*, vol. 35, Sep. 2023, doi: 10.1016/j.segan.2023.101080.
[6] ENTSO-E, "Frequency Stability Evaluation Criteria for the Synchronous Zone of Continental Europe - Requirements and Impacting Factors," *ENTSO-e Publ.*, p. 25, 2016, [Online]. Available: https://docstore.entsoe.eu/Documents/SOC documents/RGCE_SPD_frequency_stability_criteria_v10.pdf.
[7] A. J. Roscoe, G. M. Burt, and C. G. Bright, "Avoiding the non-detection zone of passive loss-of-mains (islanding) relays for synchronous generation by using low bandwidth control loops and controlled reactive power mismatches," *IEEE Trans. Smart Grid*, vol. 5, no. 2, pp. 602–611, 2014, doi: 10.1109/TSG.2013.2279016.
[8] M. R. Alam, K. M. Muttaqi, and A. Bouzerdoum, "A multifeature-based approach for islanding detection of DG in the subcritical region of vector surge relays," *IEEE Trans. Power Deliv.*, vol. 29, no. 5, pp. 2349–2358, 2014, doi: 10.1109/TPWRD.2014.2315839.
[9] K. Mäki, A. Kulmala, S. Repo, and P. Järventausta, "Problems related to islanding protection of distributed generation in distribution network," in *2007 IEEE Lausanne POWERTECH, Proceedings*, 2007, pp. 467–472, doi: 10.1109/PCT.2007.4538362.
[10] M. W. Altaf, M. T. Arif, S. Saha, S. N. Islam, M. E. Haque, and A. M. T. Oo, "Effective ROCOF-Based Islanding Detection Technique for Different Types of Microgrid," *IEEE Trans. Ind. Appl.*, vol. 58, no. 2, pp. 1809–1821, 2022, doi: 10.1109/TIA.2022.3146094.
[11] J. C. M. Vieira, D. S. Correa, W. Freitas, and W. Xu, "Performance curves of voltage relays for islanding detection of distributed generators," *IEEE Trans. Power Syst.*, vol. 20, no. 3, pp. 1660–1662, 2005, doi: 10.1109/TPWRS.2005.852128.
[12] W. Freitas, W. Xu, C. M. Affonso, and Z. Huang, "Comparative analysis between ROCOF and vector surge relays for distributed generation applications," *IEEE Trans. Power Deliv.*, vol. 20, no. 2 II, pp. 1315–1324, 2005, doi: 10.1109/TPWRD.2004.834869.
[13] I. Biyya, Z. Oubrahim, and A. Abbou, "Frequency and ROCOF estimation under steady-state and dynamic conditions for three-phase grid-connected converters," *Electr. Power Syst. Res.*, vol. 224, Nov. 2023, doi: 10.1016/j.epsr.2023.109723.
[14] I. Biyya, Z. Oubrahim, and A. Abbou, "Fast hybrid islanding detection for DGs with inverters using maximum likelihood-based ROCOF and SFS," *Comput. Electr. Eng.*, vol. 116, May 2024, doi: 10.1016/j.compeleceng.2024.109176.
[15] D. A. Ferreira, P. M. de Almeida, H. L. M. Monteiro, T. T. Cardoso, L. R. M. Silva, and C. A. Duque, "Plug-in active ROCOF method for islanding detection based on small-signal injection," *Electr. Power Syst. Res.*, vol. 201, Dec. 2021, doi: 10.1016/j.epsr.2021.107526.
[16] A. Karpilow, A. Derviškadić, G. Frigo, and M. Paolone, "Step detection in power system waveforms for improved RoCoF and frequency estimation," *Electr. Power Syst. Res.*, vol. 212, Nov. 2022, doi: 10.1016/j.epsr.2022.108527.
[17] I. Alcaide-Godinez, E. F. Areed, and R. Castellanos, "Fast Frequency Response Effect on RoCoF for Networks with Solar PV Integration," *2021 IEEE PES Innov. Smart Grid Technol. - Asia, ISGT Asia 2021*, pp. 1–5, 2021, doi: 10.1109/ISGTASIA49270.2021.9715697.
[18] H. T. Nguyen, G. Yang, A. H. Nielsen, and P. H. Jensen, "Frequency stability enhancement for low inertia systems using synthetic inertia of wind power," *IEEE Power Energy Soc. Gen. Meet.*, vol. 2018-Janua, pp. 1–5, 2018, doi: 10.1109/PESGM.2017.8274566.
[19] L. Ruttledge and D. Flynn, "Emulated inertial response from wind turbines: Gain scheduling and resource coordination," *IEEE Trans. Power Syst.*, vol. 31, no. 5, pp. 3747–3755, 2016, doi: 10.1109/TPWRS.2015.2493058.
[20] L. Huang, H. Xin, Z. Wang, L. Zhang, K. Wu, and J. Hu, "Transient Stability Analysis and Control Design of Droop-Controlled Voltage Source Converters Considering Current Limitation," *IEEE Trans. Smart Grid*, vol. 10, no. 1, pp. 578–591, 2019, doi: 10.1109/TSG.2017.2749259.
[21] K. Swierczynski, M. Habrych, and B. Brusilowicz, "A Novel Method of Vector Shift Criterion Utilization in Power System Automation," *IEEE Access*, vol. 11, no. March, pp. 38301–38308, 2023, doi: 10.1109/ACCESS.2023.3267389.
[22] G. Frigo, "Rate of Change of Frequency Measurement Challenges and Potential Applications," *Swiss Fed. Inst. Metrol.*, 2020.
[23] F. Gonzalez-Longatt, J. M. Roldan-Fernandez, H. R. Chamorro, S. Arnaltes, and J. L. Rodriguez-Amenedo, "Investigation of inertia response and rate of change of frequency in low rotational inertial scenario of synchronous dominated system," *Electron.*, vol. 10, no. 18, 2021, doi: 10.3390/electronics10182288.
[24] H. Yin *et al.*, "Precise ROCOF estimation algorithm for low inertia power grids," *Electr. Power Syst. Res.*, vol. 209, Aug. 2022, doi: 10.1016/j.epsr.2022.107968.
[25] J. A. Barrios-Gomez, F. Sanchez, G. Claudio, F. Gonzalez-Longatt, M. Acosta, and D. Topic, "RoCoF Calculation Using Low-Cost Hardware in the Loop: Multi-area Nordic Power System," *Proc. 2020 Int. Conf. Smart Syst. Technol. SST 2020*, no. November, pp. 187–192, 2020, doi: 10.1109/SST49455.2020.9264119.
[26] J. Kour and A. Shukla, "Inertia Estimation Techniques in a Solar PV Integrated Distribution System," *2023 IEEE IAS Glob. Conf. Renew. Energy Hydrog. Technol. GlobConHT 2023*, pp. 1–6, 2023, doi: 10.1109/GlobConHT56829.2023.10087696.
[27] L. Yu, X. Sun, T. Li, H. Zhong, M. Li, and Y. Shao, "Virtual Inertia Control and Identification Method of Inertia Parameters for Doubly-Fed Units," *2022 4th Int. Conf. Smart Power Internet Energy Syst. SPIES 2022*, pp. 958–963, 2022, doi: 10.1109/SPIES55999.2022.10082664.
[28] European Commission, "Commission Regulation (EU) 2017/2196 establishing a network code on electricity emergency and restoration," *Off. J. Eur. Union*, vol. 2017, no. November, pp. 312/6-312/53, 2017, [Online]. Available: https://eur-lex.europa.eu/legal-content/EN/TXT/?uri=uriserv:OJ.L_.2017.312.01.0006.01.ENG&toc=OJ:L:2017:312:TOC#d1e2376-6-1.
[29] P. Kundur, *Power System Stability and Control*. Electric Power Research Institute, 1994.

[30] E. W. Kimbark, *Power System Stability*. Wiley-IEEE Press; 1st edition, 1995.

[31] I. Report, "Continental Europe Synchronous Area Separation on 8 January 2021," *ENTSO-E*, no. February, 2021.

[32] G. A. Munoz-Hernandez, S. P. Mansoor, and D. I. Jones, *Power system dynamics*, no. 9781447122906. 2013.

[33] N. Sisakyan, G. Chilingaryan, A. Manukyan, and A. S. Mukasyan, "Combustion Synthesis of Materials for Application in Supercapacitors: A Review," *Nanomaterials*, vol. 13, no. 23. 2023, doi: 10.3390/nano13233030.

[34] K. Xu, Y. Guo, G. Lei, and J. Zhu, "A Review of Flywheel Energy Storage System Technologies," *Energies*, vol. 16, no. 18. 2023, doi: 10.3390/en16186462.

[35] F. Nadeem, S. M. S. Hussain, P. K. Tiwari, A. K. Goswami, and T. S. Ustun, "Comparative Review of Energy Storage Systems, Their Roles, and Impacts on Future Power Systems," *IEEE Access*, vol. 7, pp. 4555–4585, 2019, doi: 10.1109/ACCESS.2018.2888497.

[36] J. Mitali, S. Dhinakaran, and A. A. Mohamad, "Energy storage systems: a review," *Energy Storage Sav.*, vol. 1, no. 3, pp. 166–216, 2022, doi: https://doi.org/10.1016/j.enss.2022.07.002.

[37] E. Union, "Commission Regulation (EU) 2017/1485 of 2 August 2017 establishing a guideline on electricity transmission system operation," *Off. J. Eur. Union*, vol. 60, no. February, pp. 1–169, 2017.

[38] IEEE Std 1547, *IEEE Standard for Interconnection and Interoperability of Distributed Energy Resources with Associated Electric Power Systems Interfaces*. 2018.